Computational Materials Science 121 (2016) 1–5

Contents lists available at ScienceDirect

Computational Materials Science

journal homepage: www.elsevier.com/locate/commatsci

First-principles study of the effect of boron on grain boundary in NiAl

Fan Ji [a,b], Shang-Yi Ma [a,*], Tong-Zheng Xin [b,c], Shao-Qing Wang [a]

[a] Shenyang National Laboratory for Materials Science, Institute of Metal Research, Chinese Academy of Sciences, Shenyang 110016, China
[b] University of Chinese Academy of Science, Beijing 100049, China
[c] Department of Superalloy, Institute of Metal Research, Chinese Academy of Science, Shenyang 110016, China

ARTICLE INFO

Article history:
Received 6 February 2016
Received in revised form 15 April 2016
Accepted 17 April 2016
Available online 4 May 2016

Keywords:
Segregated B
Strengthening effect
GB cohesion
NiAl

ABSTRACT

The grain boundary (GB) is critical to the mechanical properties of NiAl. The addition of B in NiAl can lead to the increase of yield strength due to its segregation in GB. To elucidate the B-induced enhancement of GB, we investigate the segregation state and its strengthening mechanism of the additive B in the typical $\sum5(310)[001]$ GB of NiAl at atomic scale using the first-principles method. Our calculations shown that the additive B atom prefers to segregate at the interstitial *I*1 site of GB, in which case it is surrounded by four first-nearest-neighboring (1NN) and two second-nearest-neighboring (2NN) Ni atoms. It is found the segregated B prefers to bond with its neighboring Ni instead of Al atoms. Our calculations further shown not only the intergranular cohesion is improved by the covalent bonding between the segregated B and its four 1NN Ni atoms, but also the intra-planar cohesion of GB is enhanced by the covalent bonding between the segregated B and its two 2NN Ni atoms. The covalent bonding between B and Ni atoms mainly stem from the contribution of B-*p* and Ni-*d* states, partly from the weak interactions of B-*s* and Ni-*s* states. Our first-principles tensile test shown that the yield stress and ductility of NiAl are indeed improved due to the segregation of B in GB.

1. Introduction

The B2 ordered NiAl intermetallic, which has remarkable properties of low density, good oxidation and corrosion resistibility, and high melting point, is a promising candidate for high-temperature structural materials [1]. However, the intrinsic brittleness of NiAl at low temperature limits its applications in the field of aero-engine manufacturing [2]. Regarding to the brittleness, grain boundary (GB) is considered as the frail zone of NiAl. It was reported that the intergranular cohesion of NiAl is not strong and the intergranular fracture is more likely to occur under external loads [3]. Eberhart and Vvedensky [4] attributed the intergranular fracture to the reduction of covalent bonds at the GB. Muller et al. [5] suggested that the weakness of the GB stems from the changes of the *d* states of Ni near GB in comparison with that of Ni in bulk. Pankhurst et al. [6] further proposed that the broken Ni-*d* symmetries split by the *sp*–*d* hybridization result in the cohesion reduction of atom-rearranged GB.

The addition of alloying elements is an effective method to improve the mechanical properties of intermetallic. These heterogeneous additive elements not only strengthen the matrix [7,8], but also significantly enhance the intergranular cohesion due to their segregation in GB [9]. However, not all additive elements are "good" ones that have a tendency to segregate in GB and then enhance the GB cohesion [10]. For example, carbon hardly segregates in the GB of NiAl [11], while the segregated impurities like sulfur and oxygen are detrimental to GB. It was reported that the segregated sulfur may deteriorate the interfacial strength and induce the embrittlement of Ni $\sum5(012)$ GB [12–14]. In NiAl, it was found oxygen prefers to occupy the interstitial site of various $\sum5$ GBs, and then form Al_2O_3-like bonding clusters with its nearest Al atoms, which can embrittle the GB [15]. Additionally, it was suggested that the substitutional or interstitial silicon in GB has different effects on the fracture modes of Al $\sum5(012)$ GB [16]. Boron is deemed to be a potent strengthener in various alloy systems. In past years, considerable efforts have been devoted to study the effects of B-induced cohesion enhancement of GB and its strengthening mechanism in various metals and alloys. Kart et al. presented that more additive B atoms can lead to the cohesion enhancement of Ni $\sum5(012)$ GB [17]. The similar B-induced enhancement can also be observed in $\sum5(310)$ GB of Cu and FeAl systems [18,19]. In γ-Fe system, Li et al. theoretically demonstrated that B indeed acts as the GB enhancer, but some alloying elements, such as Cr, Ni, Mn, Co and Mo, can impair the enhancement of B on GB cohesion [20]. Experimentally, it was reported that the B segregated in

* Corresponding author.
E-mail address: shyma@imr.ac.cn (S.-Y. Ma).

http://dx.doi.org/10.1016/j.commatsci.2016.04.024
0927-0256/

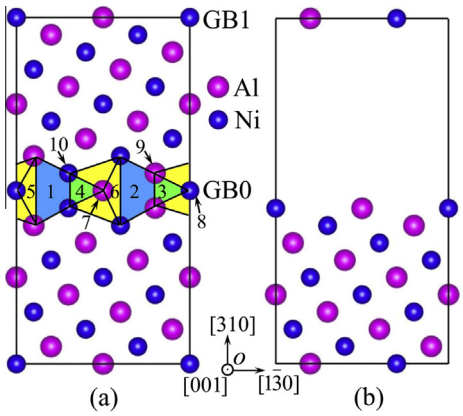

Fig. 1. The [001] direction view of the supercell model of (a) GB and (b) FS. The numerals of 1–6 and 7–10 correspond to the interstitial *I*1–*I*6 and substitutional *S*7–*S*10 sites, respectively. The interstitial sites are classified into three typical sites, the blue-, green-, yellow-filled zones denote the pentahedron, tetrahedron, and octahedron interstices, respectively. (For interpretation of the references to color in this figure legend, the reader is referred to the web version of this article.)

GB can suppress the GB embrittlement, thereby changing the GB fracture mode from intergranular to transgranular cleavage in FeAl, Ni_3Al and NiAl systems [11,21–23]. In FeAl intermetallic, Raulot et al. demonstrated that the segregated B in GB hardly bonds with Al atom but interacts strongly with neighbor Fe atoms [19]. Sun et al. pointed out that localized *p*–*d* bonding density between B and Ni may consolidate the GB in Ni_3Al [24]. To our knowledge, the study of B-induced enhancement of GB in NiAl is rare in theory, and the role played by the segregated B underlying the GB enhancement in NiAl and its explicit segregation configuration are not well understood at atomic scale. Due to the limitation of embedded atom calculation, the theoretical study of Chen et al. [25] argued that the segregated B would not strengthen the GB, which is in contrast to the available experimental results.

In this work, we employed first-principles method to investigate the effect of additive B on the cohesion of the symmetrical tilt $\sum5(310)[001]$ GB in NiAl at atomic scale. In particular, the segregation behavior and the segregated state of the additive B atom were explored in detail. Our calculations shown that the additive B has a strong tendency to segregate at the *I*1-site of the GB in NiAl. It was found that the segregated B leads to the charge redistribution in the GB region, thus gives rise to the cohesion improvement of the GB.

2. Models and computational method

Our first-principles calculations were performed with density functional theory (DFT) as implemented in the Vienna Ab-initio Simulation Package (VASP) [26]. Electron–ion interactions were described by the projected-augmented plane-wave (PAW) [27] method and the exchange–correlation interactions were treated within the Perdew–Burke–Emzerhof (PBE) generalized gradient approximation (GGA) [28]. The wave functions were expanded in a plane-wave basis set with a cutoff energy of 340 eV. The convergence criteria for energy and force were 10^{-5} eV and 0.03 eV $Å^{-1}$, respectively.

The bulk NiAl supercell was built with the size of $11.564 \times 11.564 \times 11.564$ $Å^3$ for the calculation of the segregation energy. And the corresponding Monkhorst–Pack *k*-point meshes which were used to sample the Brillouin zone of the supercell are $3 \times 3 \times 3$. It was reported that the grain boundary $\sum5$ have good crack resistance and there is a high fraction of $\sum5$ in NiAl [29]. In our calculations, the specific $\sum5(310)[001]$ symmetrical tilt boundary was constructed using the supercell model by rotating a grain around the [001] axis about 36.9° according to the coincidence site lattice (CSL) theory, as shown in Fig. 1(a). It is seen that the $\sum5$ supercell consists of two grains that contains ten (310) layers, thus two $\sum5(310)[001]$ GB, the in-between GB0 and the boundary GB1 were generated. The symmetrical first-nearest layers of the GB0 were defined as layer 1/−1. Two groups of sites for the segregated B, interstitial (*I*) and substitutional (*S*) sites, were examined in our calculations. The various possible *I* and *S* sites were denoted as *I*1–*I*6 and *S*7–*S*10, respectively. The six *I* sites (*I*1–*I*6) can be classified into three typical configurations: pentahedron, tetrahedron and octahedron interstices, which are distinguished by different filled colors in Fig. 1(a). And two types of *S* sites (*S*7–*S*10) for the substituted Ni and Al atoms in GB and in layer 1/−1 were considered. These various atomic configurations would be described in details in the following discussions. The (310) free surfaces (FS) model, as shown in Fig. 1(b), was also constructed using the slab model. The identical *I* (*I*1–*I*6) and *S* sites (*S*7–*S*10) at FS were also considered. Two groups of GB and FS supercell models corresponding to low and high B concentration were designed in our calculations to evaluate the segregated B–B interactions on the effects of GB. The sizes of the supercell model for low and high B concentrations are $8.673 \times 9.142 \times 18.284$ and $2.891 \times 9.142 \times 18.284$ $Å^3$, respectively. And the corresponding Monkhorst–Pack k-point meshes are $16 \times 4 \times 2$ and $4 \times 4 \times 2$, respectively.

Both non-spin-polarized and spin-polarized calculations had been tested before the serious calculations. However, it was found

Table 1
Various atomic configurations of *I* and *S* sites for the segregated B before and after configuration optimization, and the corresponding binding energies for the low and high B concentrations. The first- and second-nearest-neighboring atoms of the segregated B are denoted as 1NN and 2NN, respectively. The atomic configurations for the segregated B before and after relaxations are denoted as pentahedron (P), tetrahedron (T), octahedron (O) interstices and substituted (S) sites.

Position	Before relaxation		After relaxation		$E_b^{B\text{-doped}}$(GB) (eV)	
					Low B	High B
*I*1	4 Ni (1NN), 2 Al (2NN)	P	4 Ni (1NN), 2 Ni (2NN)	P	−7.20	−7.00
*I*2	4 Al (1NN), 2 Ni (2NN)	P	2 Ni (1NN), 4 Al (2NN)	P	−6.16	−5.96
*I*3	2 Al (1NN), 2 Ni (2NN)	T	2 Ni (1NN), 2 Al (2NN)	O	−4.11	−5.04
*I*4	2 Ni (1NN), 2 Al (2NN)	T	1 Ni (1NN), 2 Ni (2NN)	O	−4.89	−5.75
*I*5	2 Ni (1NN), 4 Al (2NN)	O	2 Ni (1NN), 2 Al (2NN)	O	−4.11	−5.04
*I*6	2 Al (1NN), 4 Ni (2NN)	O	1 Ni (1NN), 2 Ni (2NN)	O	−4.89	−5.75
*S*7	8 Ni	S	4 Ni (1NN), 4 Ni (2NN)	S	−1.65	−0.92
*S*8	8 Al	S	4 Al (1NN), 4 Al (2NN)	S	0.64	1.00
*S*9	1 Al (1NN), 6 Ni (2NN)	S	6 Ni	S	−2.26	−2.55
*S*10	1 Ni (1NN), 6 Al (2NN)	S	1 Ni (1NN), 2 Ni (2NN)	S	0.15	−0.34